

Inflation due to a non-minimal coupling of singlet scalars in the radiative seesaw model

Romy H. S. Budhi ^{*,†,1}, Shoichi Kashiwase ^{†,2},
and
Daijiro Suematsu ^{†,3}

^{}Physics Department, Gadjah Mada University, Yogyakarta 55281, Indonesia*

[†]Institute for Theoretical Physics, Kanazawa University, Kanazawa 920-1192, Japan

Abstract

The radiative neutrino mass model with inert doublet dark matter is a promising model for the present experimental issues which cannot be explained within the standard model. We study an extension of this model focusing on cosmological features brought about from the scalar sector. Inflation due to singlet scalars with hierarchical non-minimal couplings with the Ricci scalar may give a favorable solution for both neutrino masses and baryon number asymmetry in the Universe.

¹e-mail: romyhanang@hep.s.kanazawa-u.ac.jp, romyhanang@ugm.ac.id

²e-mail: shoichi@hep.s.kanazawa-u.ac.jp

³e-mail: suematsu@hep.s.kanazawa-u.ac.jp

1 Introduction

Recent discovery of the Higgs particle [1] suggests that the framework of the standard model (SM) can describe Nature up to the weak scale. On the other hand, we have several experimental results which are not explained within it. Representative ones are the existence of both small neutrino masses [2] and dark matter (DM) [3], and also the baryon number asymmetry in the Universe [4]. These require some extension of the SM.

As such an extension, we have an interesting simple model, in which the SM is extended by an inert doublet scalar and singlet fermions [5]. It has promising features for the simultaneous explanation of the neutrino oscillation data [2] and the observed abundance of DM [3] through physics at TeV regions. In fact, if these new fields are assigned odd parity of an imposed Z_2 symmetry, the neutrino masses are generated at one-loop level and the lightest Z_2 odd particle can behave as DM. The quantitative conditions required for their explanation and also other phenomenological aspects have been extensively studied in this model and its extended models [6, 7, 8, 9, 10, 11]. They show that the simultaneous explanation of these is possible without causing strong tension with other phenomena like lepton flavor violating processes as long as DM is identified with the lightest neutral component of the inert doublet scalar [11, 12].⁴ Moreover, in that case, the baryon number asymmetry in the Universe could be also successfully explained if rather mild mass degeneracy is assumed among the singlet fermions with masses of TeV scales [11].

In this paper, we consider how inflation can be embedded in this framework. CMB observations [13, 14, 15] suggest that the exponential expansion of the Universe should occur before the ordinary Big-Bang of the Universe. On the other hand, the analyses of them seem to have already ruled out a lot of inflation models proposed by now. Higgs inflation is a well-known example which is still alive [16]. This model is characterized by the feature such that Higgs potential becomes flat enough for large field regions if the Higgs scalar has a large non-minimal coupling with the Ricci scalar. We apply this idea to a radiative seesaw model extended by real singlet scalars [17]. Although the singlet scalars are originally introduced with the aim of generating the neutrino masses, it could work as inflaton if they are supposed to have a substantial non-minimal coupling with the Ricci

⁴If the lightest singlet fermion is identified with DM, strong tension appears between the DM abundance and the lepton flavor violating processes [6]. However, it could be resolved by assuming special flavor structure [7] or introducing a new interaction [8].

scalar. In fact, such a coupling of a real singlet scalar has been studied as s -inflation in a different context [18]. Following it, we focus our attention on such a non-minimal coupling of the singlet scalars with the Ricci scalar instead of the one of Higgs scalar and others. In this case, unitarity problem which appears in the Higgs inflation and other general models [19, 20] might be escaped under certain conditions. Moreover, the singlet scalars could also play an important role in the generation of the baryon number asymmetry in the Universe through non-thermal leptogenesis. We study this issue intensively.

The following parts of the paper are organized as follows. In section 2, we introduce the model studied in this paper and discuss the neutrino mass generation. In section 3, a possible inflation scenario in this model is discussed. Production of the baryon number asymmetry due to the inflaton decay is studied in detail in section 4. Consistency of the DM physics with this scenario is also discussed here. Section 5 is devoted to the summary of the paper.

2 An extension with real singlet scalars

The radiative seesaw model proposed in [5] is characterized by a scalar quartic coupling $\lambda_5(\eta^\dagger\phi)^2$ between the ordinary Higgs doublet ϕ and the inert doublet scalar η . Since η and singlet fermions N_k are assigned odd parity of the Z_2 symmetry and all the SM contents are assigned even parity, the Dirac neutrino mass terms are forbidden at tree level. Neutrino masses are generated through a one-loop diagram with N_k and η in the internal lines. In this mass generation scenario at TeV scales, the above mentioned quartic coupling between ϕ and η plays an essential role to explain the small neutrino masses.

An extension of the model might be done by considering a possibility that this quartic coupling is an effective coupling appearing at low energy regions after integrating out heavy scalar fields [17]. Such a scenario could be realized by introducing Z_2 odd real singlet scalars S_a ($a = 1, 2$).⁵ The model is defined by a part of Lagrangian relevant to

⁵One real scalar is enough for the neutrino mass generation and inflation. However, if we consider leptogenesis in the model, two real scalars should be introduced at least. We take this minimal version here.

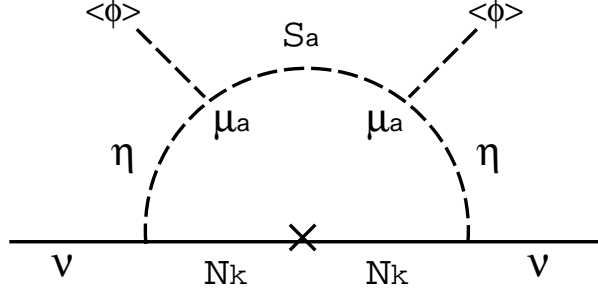


Fig. 1 The one-loop diagram which contributes neutrino mass generation in the present model.

the new fields as follows,

$$\begin{aligned}
-\mathcal{L} = & \sum_{\alpha,k=1}^3 \left[h_{\alpha k} \bar{N}_k \eta^\dagger \ell_\alpha + h_{\alpha k}^* \bar{\ell}_\alpha \eta N_k + \frac{M_k}{2} \bar{N}_k N_k^c + \frac{M_k}{2} \bar{N}_k^c N_k \right] \\
& + m_\phi^2 \phi^\dagger \phi + m_\eta^2 \eta^\dagger \eta + \lambda_1 (\phi^\dagger \phi)^2 + \lambda_2 (\eta^\dagger \eta)^2 + \lambda_3 (\phi^\dagger \phi) (\eta^\dagger \eta) + \lambda_4 (\eta^\dagger \phi) (\phi^\dagger \eta) \\
& + \sum_{a=1,2} \left[\frac{m_{S_a}^2}{2} S_a^2 + \frac{\kappa_1^{(a)}}{4} S_a^4 + \frac{\kappa_2^{(a)}}{2} S_a^2 (\phi^\dagger \phi) + \frac{\kappa_3^{(a)}}{2} S_a^2 (\eta^\dagger \eta) + \mu_a S_a \eta^\dagger \phi + \mu_a^* S_a \phi^\dagger \eta \right],
\end{aligned} \tag{1}$$

where ℓ_α is a left-handed doublet lepton. We note that $\lambda_5 (\eta^\dagger \phi)^2$ is allowed under the imposed symmetry in general. However, if we assume $\lambda_5 = 0$ in the original Lagrangian, its β -function is proportional to itself and then $\lambda_5 = 0$ is stable against the radiative correction as long as μ_a terms are not included in eq. (1). On the other hand, if the μ_a terms are introduced in eq. (1) assuming $\lambda_5 = 0$, the λ_5 term appears effectively as discussed below. Later, this point will be discussed again in relation to the assignment of lepton number to the new fields.

In this model, neutrino masses are generated through a one-loop diagram which is shown in Fig. 1. They are estimated as

$$\mathcal{M}_{\alpha\beta}^\nu = \sum_{k=1}^3 \frac{h_{\alpha k} h_{\beta k} M_k \langle \phi \rangle^2}{8\pi^2} \sum_a \mu_a^2 I(M_\eta, M_k, m_{s_a}), \tag{2}$$

where $M_\eta^2 = m_\eta^2 + (\lambda_3 + \lambda_4) \langle \phi \rangle^2$ and $\langle \phi \rangle = 174$ GeV. The function I is defined by

$$\begin{aligned}
I(m_a, m_b, m_c) = & \frac{(m_a^4 - m_b^2 m_c^2) \ln m_a^2}{(m_b^2 - m_a^2)^2 (m_c^2 - m_a^2)^2} + \frac{m_b^2 \ln m_b^2}{(m_c^2 - m_b^2) (m_a^2 - m_b^2)^2} \\
& + \frac{m_c^2 \ln m_c^2}{(m_b^2 - m_c^2) (m_a^2 - m_c^2)^2} - \frac{1}{(m_b^2 - m_a^2) (m_c^2 - m_a^2)}.
\end{aligned} \tag{3}$$

If we suppose $m_{S_a} \gg M_\eta, M_k$, this formula can be approximated as

$$\mathcal{M}_{\alpha\beta}^\nu = \sum_a \frac{\mu_a^2}{m_{S_a}^2} \sum_{k=1}^3 \frac{h_{\alpha k} h_{\beta k} \langle \phi \rangle^2}{8\pi^2} \frac{M_k}{M_\eta^2 - M_k^2} \left[\frac{M_k^2}{M_\eta^2 - M_k^2} \ln \frac{M_k^2}{M_\eta^2} + 1 \right]. \quad (4)$$

This is equivalent to the neutrino mass formula in the original model if $\sum_a \frac{\mu_a^2}{m_{S_a}^2}$ is identified with the quartic coupling constant λ_5 [17]. This correspondence could be directly confirmed in an effective model at energy regions smaller than m_{S_a} , which can be derived by integrating out S_a . In fact, since the equation of motion for S_a could be approximated as $S_a \simeq -\frac{1}{m_{S_a}^2}(\mu_a \eta^\dagger \phi + \mu_a^* \phi^\dagger \eta)$, the required terms are derived by using it as

$$-\frac{1}{2} \sum_a \left[\frac{\mu_a^2}{m_{S_a}^2} (\eta^\dagger \phi)^2 + \frac{\mu_a^{*2}}{m_{S_a}^2} (\phi^\dagger \eta)^2 \right]. \quad (5)$$

Origin of the smallness of $|\lambda_5|$, which is a key to explain the small neutrino masses in the original model, is translated to the hierarchy problem between μ_a and m_{S_a} in this scenario. We cannot answer the origin of this hierarchy at the present stage and we have to leave it for a complete theory at high energy regions.

For the later study, we show an example of flavor structure of the neutrino Yukawa couplings which can explain every neutrino oscillation data in the normal hierarchy case. Here, we follow the procedure given in [11]. For this purpose, we assume that the neutrino mass matrix (4) takes the following simple form as

$$\mathcal{M}^\nu = \begin{pmatrix} 0 & 0 & 0 \\ 0 & 1 & q_1 \\ 0 & q_1 & q_1^2 \end{pmatrix} (h_1^2 \Lambda_1 + h_2^2 \Lambda_2) \frac{\mu_2^2}{m_{S_2}^2} + \begin{pmatrix} 1 & q_2 & -q_3 \\ q_2 & q_2^2 & -q_2 q_3 \\ -q_3 & -q_2 q_3 & q_3^2 \end{pmatrix} h_3^2 \Lambda_3 \frac{\mu_2^2}{m_{S_2}^2}, \quad (6)$$

where $\frac{|\mu_1|^2}{m_{S_1}^2} \ll \frac{|\mu_2|^2}{m_{S_2}^2}$ is assumed⁶ and Λ_k is represented as

$$\Lambda_k = \frac{\langle \phi \rangle^2}{8\pi^2 \text{ GeV}} \frac{\frac{1\text{GeV}}{M_k}}{\frac{M_\eta^2}{M_k^2} - 1} \left[1 + \frac{M_k^2}{M_\eta^2 - M_k^2} \ln \frac{M_k^2}{M_\eta^2} \right] \equiv \frac{\langle \phi \rangle^2}{8\pi^2 \text{ GeV}} \tilde{\Lambda}_k. \quad (7)$$

If we put $q_{1,2,3} = 1$ in eq. (6), the Pontecorvo-Maki-Nakagawa-Sakata (PMNS) mixing matrix is found to reduce to the tri-bimaximal form

$$U_{PMNS} = \begin{pmatrix} \frac{2}{\sqrt{6}} & \frac{1}{\sqrt{3}} & 0 \\ \frac{-1}{\sqrt{6}} & \frac{1}{\sqrt{3}} & \frac{1}{\sqrt{2}} \\ \frac{1}{\sqrt{6}} & \frac{-1}{\sqrt{3}} & \frac{1}{\sqrt{2}} \end{pmatrix} \begin{pmatrix} 1 & 0 & 0 \\ 0 & e^{i\alpha_1} & 0 \\ 0 & 0 & e^{i\alpha_2} \end{pmatrix}, \quad (8)$$

⁶As explained in the later discussion, this assumption is adopted in connection with leptogenesis.

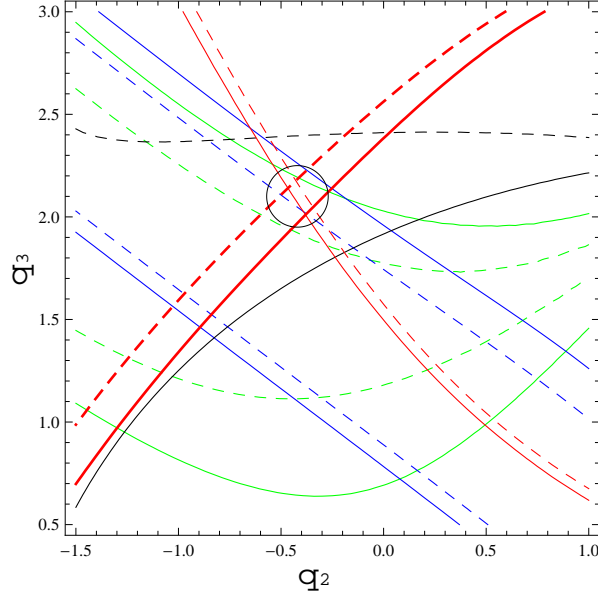


Fig. 2 A region in the (q_2, q_3) plane allowed by the neutrino oscillation data, which is included inside a circle drawn by the black solid line. Other parameters are fixed to satisfy the condition (10). Each contour represents 2σ boundary values of neutrino oscillation parameters [21], that is, $|\Delta m^2_{32}|$ (thick red solid and dashed lines), Δm^2_{21} (thin red solid and dashed lines), $\sin^2 2\theta_{23}$ (green solid and dashed lines), $\sin^2 2\theta_{12}$ (blue solid and dashed lines) and $\sin^2 2\theta_{13}$ (black solid and dashed lines).

where Majorana phases $\alpha_{1,2}$ are determined by the phases h_i and μ_a . If we put $\varphi_i = \arg(h_i)$ and $\varphi_{\mu_a} = \arg(\mu_a)$, they are expressed as

$$\alpha_1 = \varphi_3 + \varphi_{\mu_2}, \quad \alpha_2 = \varphi_2 + \varphi_{\mu_2}, \quad (9)$$

where $|h_1|$ is taken as a negligibly small value compared with others, for simplicity.⁷ Since one of mass eigenvalues is always zero in this flavor structure, we find that the mass eigenvalues should satisfy $|h_2|^2 \Lambda_2 \frac{|\mu_2|^2}{m_{S_2}^2} \simeq \frac{\sqrt{\Delta m_{\text{atm}}^2}}{2}$ and $|h_3|^2 \Lambda_3 \frac{|\mu_2|^2}{m_{S_2}^2} \simeq \frac{\sqrt{\Delta m_{\text{sol}}^2}}{3}$, where Δm_{atm}^2 and Δm_{sol}^2 stand for the squared mass differences required by the neutrino oscillation analysis for both atmospheric and solar neutrinos [2, 21].

Since we now know that $\sin \theta_{13}$ takes a non-zero value, we have to consider a flavor structure deviated from $q_{1,2,3} = 1$. For that purpose, we determine values of $q_{1,2,3}$, $h_2^2 \tilde{\Lambda}_2 \frac{|\mu_2|^2}{m_{S_2}^2}$ and $h_3^2 \tilde{\Lambda}_3 \frac{|\mu_2|^2}{m_{S_2}^2}$ to realize all the squared mass differences and the mixing angles required

⁷The model is equivalent to the one with two singlet fermions in this case. It should be noted that the neutrino oscillation data could be explained as long as only two singlet fermions are introduced. We use this setting throughout the following study.

$M_\eta(\text{GeV})$	$\frac{ \mu_1 }{m_{S_1}}$	$\frac{ \mu_2 }{m_{S_2}}$	h_2	h_3	$M_2(\text{GeV})$	$M_3(\text{GeV})$	$ Y_B $
10^3 (a)	$2 \cdot 10^{-5}$	10^{-3}	$1.12 \cdot 10^{-2}$	$5.13 \cdot 10^{-3}$	$5.30 \cdot 10^3$	$9.00 \cdot 10^3$	$1.3 \cdot 10^{-9}$
(b)	$2 \cdot 10^{-6}$	$8 \cdot 10^{-2}$	$8.40 \cdot 10^{-3}$	$3.85 \cdot 10^{-3}$	$1.73 \cdot 10^8$	$2.19 \cdot 10^8$	$3.5 \cdot 10^{-10}$
600	$2 \cdot 10^{-5}$	10^{-3}	$9.62 \cdot 10^{-3}$	$4.54 \cdot 10^{-3}$	$5.30 \cdot 10^3$	$9.00 \cdot 10^3$	$5.1 \cdot 10^{-10}$
$3 \cdot 10^3$	$2 \cdot 10^{-5}$	10^{-3}	$2.15 \cdot 10^{-3}$	$8.94 \cdot 10^{-3}$	$2.67 \cdot 10^4$	$2.77 \cdot 10^4$	$3.4 \cdot 10^{-9}$

Table 1 Examples of the model parameters which satisfy the latter two conditions in eq. (10). If we fix a point in a circle of Fig. 2, all the neutrino oscillation data can be explained at 2σ level, consistently. In all cases, $m_{S_1} = 10^9$ GeV and $\frac{m_{S_2}}{m_{S_1}} = 1.1$ are assumed.

by the neutrino oscillation data through diagonalizing the matrix (6) numerically. This analysis shows that the neutrino oscillation parameters can be in the 2σ range of the experimental data if the values of (q_2, q_3) are contained in the region surrounded by a circle in Fig. 2. In this figure, the remaining parameters are fixed so as to satisfy

$$q_1 = 0.77, \quad h_2^2 \tilde{\Lambda}_2 \frac{|\mu_2|^2}{m_{S_2}^2} = 6.03 \times 10^{-14}, \quad h_3^2 \tilde{\Lambda}_3 \frac{|\mu_2|^2}{m_{S_2}^2} = 1.02 \times 10^{-14}. \quad (10)$$

As long as the model parameters $\frac{\mu_2}{m_{S_2}}$, M_η , $h_{2,3}$ and $M_{2,3}$ are varied by keeping these conditions, the neutrino oscillation constraints are automatically fulfilled. In Table 1, typical examples obtained by this simple procedure are shown. They include examples such that the masses of the singlet fermions M_k are largely different in the case $M_\eta = 1$ TeV, in which they are of $O(10^4)$ GeV and $O(10^8)$ GeV in the cases (a) and (b), respectively.

If S_a does not play any other role than the neutrino mass generation, this extension may not be so appealing. However, we can find that the introduction of S_a could add favorable features as an inflation model to the radiative seesaw model.⁸ Recent Planck data suggest that the Higgs inflation scenario could be one of the favored inflation models. However, if multi-component scalars like the Higgs doublet scalar are supposed to play a role of inflaton, the model could be suffered from the unitarity problem [19, 20]. Since unitarity could be violated in the scattering amplitudes among scalars with non-minimal

⁸We have proposed another inflation scenario in the similar context based on somewhat different motivation in [22]. The inflaton potential assumed there differs from the present one. As a result, the predicted values for the spectral index and the tensor-to-scalar ratio take distinct values from the present ones.

couplings to the Ricci scalar at a lower scale compared with the inflation scale, new physics required for unitarity restoration could jeopardize the flatness of inflaton potential at the inflation scale. The situation can be changed in a real singlet inflaton as discussed in [20]. In the following part, we consider that only the singlet scalars among scalars in the model have non-negligible non-minimal couplings with the Ricci scalar.

3 Inflation due to the non-minimal coupling

It has been known that a scalar field coupled with the Ricci scalar can bring about the exponential expansion of the Universe [23]. Using this idea to the SM, Higgs inflation has been proposed in [16] as a scenario with a realistic inflaton candidate. After that, the scenario has been studied from various view points [24]. We apply this idea to the singlet scalars in this model but not to the Higgs doublet or the inert doublet.⁹ The action relevant to the present inflation scenario is given in the Jordan frame as

$$S_J = \int d^4x \sqrt{-g} \left[\frac{1}{2} M_{\text{pl}}^2 R + \sum_a \frac{1}{2} \xi_a S_a^2 R + \sum_a \frac{1}{2} \partial^\mu S_a \partial_\mu S_a - V(S_a) \right], \quad (11)$$

where M_{pl} is the reduced Planck mass and $V(S_a)$ stands for the corresponding part of the S_a potential in eq. (1). We note that only the singlet scalars are assumed to have non-minimal coupling with the Ricci scalar.

We take S_1 as inflaton and other scalars are assumed to have much smaller values than S_1 during the inflation. In that case, $V(S_a)$ can be approximately expressed as $V(S_a) \simeq \frac{\kappa_1^{(1)}}{4} S_1^4$ for a sufficiently large value of S_1 , where the coupling $\kappa_i^{(1)}$ of inflaton is abbreviated as κ_i and $\kappa_1 S_1^2 \gg m_{S_1}^2$ is supposed implicitly. In order to derive the corresponding action to eq. (11) in the Einstein frame, we use the conformal transformation [16, 23]

$$g = \Omega^2 g_E, \quad \Omega^2 = 1 + \frac{\sum_a \xi_a S_a^2}{M_{\text{pl}}^2}. \quad (12)$$

As a result of this transformation, we find that it is written as

$$S_E = \int d^4x \sqrt{-g_E} \left[\frac{1}{2} M_{\text{pl}}^2 R_E + \frac{1}{2\Omega^4} \sum_{a,b=1,2} \left(\delta_{ab} + \frac{\xi_a \delta_{ab} S_a^2 + 6\xi_a \xi_b S_a S_b}{M_{\text{pl}}^2} \right) \partial^\mu S_a \partial_\mu S_b - \frac{1}{\Omega^4} V(S_a) \right]. \quad (13)$$

⁹The study of Higgs inflation in the inert doublet model can be found in [25]. Although the present inflation scenario and its prediction are essentially the same as [16, 18], we note that the inflaton is shown to play crucial roles in the neutrino mass generation and the leptogenesis in this model.

An important feature is the appearance of the mixing between $\partial_\mu S_a$ and $\partial_\mu S_b$ in the second term. We will discuss it later.

We consider a case in which only one real scalar S_1 has the non-minimal coupling with the Ricci scalar at first. In that case, a canonically normalized field χ can be introduced as

$$\frac{d\chi}{dS_1} = \frac{\left[1 + (\xi_1 + 6\xi_1^2) \frac{S_1^2}{M_{\text{pl}}^2}\right]^{1/2}}{1 + \frac{\xi_1 S_1^2}{M_{\text{pl}}^2}}. \quad (14)$$

The potential $\frac{1}{\Omega^4}V(S_1)$ can be expressed by using this χ . It is easily seen that the new field χ coincides with S_1 at the regions where $S_1 \ll \frac{M_{\text{pl}}}{\sqrt{\xi_1}}$ is satisfied. On the other hand, if S_1 takes a large value such as $S_1 \gg \frac{M_{\text{pl}}}{\sqrt{\xi_1}}$, S_1 and χ are found from eq. (14) to be related as $S_1 \propto \exp\left(\frac{\chi}{\sqrt{6+\frac{1}{\xi_1}}M_{\text{pl}}}\right)$. The potential at this region is found to be almost constant as

$$V_E^{(1)} = \frac{\kappa_1 S_1^4}{4 \left(1 + \frac{\xi_1 S_1^2}{M_{\text{pl}}^2}\right)^2} \simeq \frac{\kappa_1 M_{\text{pl}}^4}{4\xi_1^2}. \quad (15)$$

This suggests that χ could play a role of slow-rolling inflaton in this region.

The number of e-foldings induced by the potential $V_E^{(1)}$ can be estimated as

$$N = \frac{1}{M_{\text{pl}}^2} \int_{\chi_{\text{end}}}^{\chi} d\chi \frac{V_E^{(1)}}{V_E^{(1)'}} \simeq \frac{3}{4} \frac{S_1^2 - S_{1,\text{end}}^2}{M_{\text{pl}}^2/\xi_1}, \quad (16)$$

where $V_E^{(1)'} = \frac{dV_E^{(1)}}{d\chi}$ and eq. (14) is used. Slow roll parameters derived from this potential are summarized as [26]

$$\varepsilon = \frac{1}{M_{\text{pl}}^2} \left(\frac{V_E^{(1)'}}{V_E^{(1)}} \right)^2 = \frac{4M_{\text{pl}}^4}{3\xi_1^2 S_1^4}, \quad \eta = M_{\text{pl}}^2 \left(\frac{V_E^{(1)''}}{V_E^{(1)'}} \right) = -\frac{4M_{\text{pl}}^2}{3\xi_1 S_1^2}. \quad (17)$$

Since the inflation is considered to end at $\varepsilon \simeq 1$, we have $S_{1,\text{end}}^2 \simeq \sqrt{\frac{4}{3}} \frac{M_{\text{pl}}^2}{\xi_1}$, which suggests that $S_{1,\text{end}}$ could be neglected in eq. (16). Thus, the slow roll parameters are found to be expressed as $\varepsilon \simeq \frac{3}{4}N^{-2}$ and $\eta \simeq -N^{-1}$ by using the e -foldings N only.

The spectrum of density perturbation predicted by the inflation is expressed as

$$\mathcal{P}(k) = A_s \left(\frac{k}{k_*} \right)^{n_s-1}, \quad A_s = \frac{V_E^{(1)}}{24\pi^2 M_{\text{pl}}^4 \varepsilon} \Big|_{k_*}. \quad (18)$$

If we use $A_s = (2.445 \pm 0.096) \times 10^{-9}$ at $k_* = 0.002 \text{ Mpc}^{-1}$ [13], we find that the relation $\kappa_1 \simeq 10^{-6} \xi_1^2 N^{-2}$ should be satisfied at the horizon exit time of the scale k_* . The spectral

index n_s and the tensor-to-scalar ratio r are represented by using the slow-roll parameters as [26]

$$n_s = 1 - 6\varepsilon + 2\eta, \quad r = 16\varepsilon. \quad (19)$$

Using eq. (17) to these formulas, they are found to be determined only by the e -foldings N such as $n_s \sim 0.968$ and $r \sim 3.0 \times 10^{-3}$ for $N = 60$. These values coincide with the ones estimated from the Planck data well. Although all these results are the same as the ones found in the Higgs inflation, the quartic coupling κ_1 is a free parameter in this model. It is completely different from the Higgs inflation where the corresponding quartic coupling is constrained by the Higgs mass 126 GeV. As a result, we cannot relate weak scale physics to the inflation through the observational data of the Universe in this model. On the contrary, this fact allows that ξ_1 takes a much smaller value compared with the one of the usual Higgs inflation. For example, $\xi_1 = O(10^2)$ can realize both $N = 60$ and the observed value of A_s if a very small value such as $O(10^{-6})$ is assumed for κ_1 . However, as found from the expression of the slow-roll parameters which depend only on N , the predicted values for n_s and r are the same as those of the Higgs inflation.

Next, we consider the model with two real scalars, which corresponds to the one discussed in the previous section. The situation could largely change if multi-scalars have couplings with the Ricci scalar. In general, the mixing in eq. (13) cannot be resolved by any field redefinition and then it is difficult to find canonically normalized basis for them. An exceptional situation for this could be found for hierarchical couplings such as $\xi_1 \gg 1$ and $\xi_1 \xi_2 \ll 1$. This condition can be freely imposed on the present model since S_1 and S_2 are not related by any symmetry. In that case, the model could behave as a single real field model [20]. We can introduce a canonically normalized field χ for S_1 in the same way as eq. (14). On the other hand, the S_2 relevant terms in eq. (13) are strongly suppressed as long as $\xi_1 S_1^2 > M_{\text{pl}}^2$ is satisfied. In the potential V , the S_2 relevant part can be given as

$$V_E^{(2)} = \frac{\kappa_1^{(2)} S_2^4}{2 \left(1 + \frac{\xi_1 S_1^2}{M_{\text{pl}}^2}\right)^2} \simeq \frac{\kappa_1^{(2)} M_{\text{pl}}^4}{2 \xi_1^2} \left(\frac{S_2}{S_1}\right)^4 \ll V_E^{(1)}. \quad (20)$$

This means that only the χ could play a role of slow-roll inflaton also in this case.

In addition, under the condition $\xi_1 \xi_2 \ll 1$, the scale of unitarity violation could be comparable to the inflation scale $\frac{M_{\text{pl}}}{\sqrt{\xi_1}}$ [20]. The unitarity violating scattering induced by the mixing part in the second term in eq. (13) could give the strongest constraint. A

simple power counting for the scattering amplitude between S_1 and S_2 suggests that the unitarity violating scale is given by $\Lambda = \frac{M_{\text{pl}}}{\sqrt{\xi_1 \xi_2}}$. However, since the condition $\sqrt{\xi_1 \xi_2} < \sqrt{\xi_1}$ is satisfied, the unitarity violating scale Λ could be comparable to or larger than the inflation scale $\frac{M_{\text{pl}}}{\sqrt{\xi_1}}$. Since S_1 and S_2 are independent fields in the present model, $\xi_2 \ll 1$ is possible even if we assume a suitable value of ξ_1 for inflation. Other possible unitarity violation induced by other parts such as V_E might be studied through the analysis by taking account of the background field dependence. It suggests that the unitarity violation scale is comparable to the inflation scale or larger than that. Thus, the flatness of the present inflaton potential is reliable throughout the inflation period. Any physics which remedies the unitarity violation does not affect the present inflation scenario.

4 Non-thermal leptogenesis and dark matter

4.1 Leptogenesis

Reheating after inflation is another important problem for this inflation scenario to be realistic. If we impose the existence of sufficient thermal relics of the inert doublet DM η_R^0 in the present Universe, reheating temperature should be higher than its mass $M_{\eta_R^0}$ at least, which is supposed to be of $O(1)$ TeV in the present study. Since the allowed decay mode for the inflaton S_1 is limited to $S_1 \rightarrow \eta^\dagger \phi$, $\phi^\dagger \eta$, the decay width of S_1 could be estimated as $\Gamma_{S_1} = \frac{1}{8\pi} \frac{|\mu_1|^2}{m_{S_1}}$. Applying instantaneous thermalization approximation to this process, the reheating temperature could be estimated from the condition $H \simeq \Gamma_{S_1}$ as

$$T_R \simeq 1.74 g_*^{-1/4} (\Gamma_{S_1} M_{\text{pl}})^{1/2} \simeq 1.6 \times 10^{12} \left(\frac{|\mu_1|}{m_{S_1}} \right)^{1/2} \left(\frac{|\mu_1|}{10^8 \text{ GeV}} \right)^{1/2} \text{ GeV}, \quad (21)$$

where $g_* = 116$ is used. If $T_R > M_{\eta_R^0}$ is satisfied and η_R^0 exists in the thermal bath, the observed DM abundance could be explained as the relic abundance of this thermal η_R^0 . The relic abundance is discussed in the next subsection.

Several leptogenesis scenarios may be considered in this reheating processes depending on the lepton number assignment for new ingredients. First, we consider an ordinary lepton number assignment to the new fields η and N_k such that $L(\eta) = 0$ and $L(N_k) = 1$. In this case, if the reheating temperature is higher than a certain bound required for the heavy singlet fermion masses,¹⁰ the usual thermal leptogenesis could work. On the other

¹⁰As discussed in [11], this bound for the singlet fermion masses could be relaxed in the radiative seesaw

hand, if the reheating temperature is not so high but high enough to thermalize the singlet fermions with masses of $O(1)$ TeV for example, the sufficient baryon number asymmetry could be generated through the resonant leptogenesis [28, 29] as long as the masses of the singlet fermions are finely degenerate [11].

If we find that there is another possible assignment of the lepton number such as $L(\eta) = 1$ and $L(N_k) = 0$ [17, 30], we can consider a new leptogenesis scenario allowed in this model. It is based on the non-thermal generation of lepton number asymmetry through the inflaton decay.¹¹ Although the quartic coupling $\lambda_5(\eta^\dagger\phi)^2$ is forbidden by this lepton number assignment, it could be generated effectively through the lepton number violating tri-linear scalar couplings μ_a at low energy regions as discussed in the previous section. Since this coupling violates the lepton number, the decay of inflaton induced through this coupling could generate the lepton number asymmetry in the η sector through the interference between tree and one-loop processes. The CP asymmetry expected in this decay can be estimated as

$$\begin{aligned}\epsilon &\equiv \frac{\Gamma(S_1 \rightarrow \eta\phi^\dagger) - \bar{\Gamma}(S_1 \rightarrow \eta^\dagger\phi)}{\Gamma(S_1 \rightarrow \eta\phi^\dagger) + \bar{\Gamma}(S_1 \rightarrow \eta^\dagger\phi)} \\ &= \frac{|\mu_2|^2}{8\pi} \left[\frac{1}{m_{S_1}^2} \ln \frac{(m_{S_1}^2 + m_{S_2}^2)}{m_{S_2}^2} + \frac{m_{S_1}^2 - m_{S_2}^2}{(m_{S_1}^2 - m_{S_2}^2)^2 + m_{S_2}^2 \Gamma_{S_2}^2} \right] \sin 2(\theta_1 - \theta_2), \quad (22)\end{aligned}$$

where $\theta_a = \arg(\mu_a)$ and $\Gamma_{S_2} = \frac{1}{8\pi} \frac{|\mu_2|^2}{m_{S_2}}$. In the following study, we assume the maximum CP phase $|\sin 2(\theta_1 - \theta_2)| = 1$.

Since η_R^0 is supposed to be DM, all components of η is expected to be lighter than N_k . In that case, the generated lepton number asymmetry cannot be transferred from the η sector to the doublet lepton sector through the η decay.¹² However, it can be converted to the lepton sector through 2-2 scattering processes. If this conversion occurs

model in comparison with the famous Davidson-Ibarra bound in the usual seesaw model [27].

¹¹The generation of lepton number asymmetry through the inflaton decay has been considered. In [31], for example, the asymmetry is supposed to be generated by its decay to the heavy right-handed neutrinos and their successive decay in the SO(10) GUT framework. Mass of the decay products is largely different from the one in the present scenario.

¹²If a singlet fermion is considered to be DM, η could decay to the lepton and then the lepton number asymmetry in the η sector moves to the lepton sector directly through it [17]. In this case, unfortunately, the relic DM abundance could have serious tensions with the lepton flavor violating processes (LFV) [6]. However, if we assume a certain flavor structure for neutrino Yukawa couplings, the LFV constraints could be satisfied. Detailed analysis for realistic parameters will be presented elsewhere.

efficiently without inducing any contradiction with other phenomenological constraints, the sphaleron interaction is expected to generate the baryon number asymmetry from this lepton number asymmetry. It has already been studied in a different inflation scenario [30]. However, since the parameter space of the present model is much simpler than the one of that model, we can study the feature of the scenario in a systematic way. We start with a brief review for the method of the analysis at first.

The lepton number asymmetry in the co-moving volume is expressed by using the entropy density s as $\Delta Y_L \equiv \frac{n_\ell - n_{\bar{\ell}}}{s}$ in the doublet lepton sector and as $\Delta Y_\eta \equiv \frac{n_\eta - n_{\eta^\dagger}}{s}$ in the η sector, respectively. Boltzmann equations which describe the evolution of these quantities are given as

$$\begin{aligned}\frac{d\Delta Y_\eta}{dz} &= -\frac{z}{sH(M_\eta)} \left[2(\gamma_a + \gamma_b) \left(\frac{\Delta Y_\eta}{Y_\eta^{\text{eq}}} - \frac{\Delta Y_L}{Y_L^{\text{eq}}} \right) + 2(\gamma_x + \gamma_y) \frac{\Delta Y_\eta}{Y_\eta^{\text{eq}}} \right], \\ \frac{d\Delta Y_L}{dz} &= \frac{z}{sH(M_\eta)} 2(\gamma_a + \gamma_b) \left(\frac{\Delta Y_\eta}{Y_\eta^{\text{eq}}} - \frac{\Delta Y_L}{Y_L^{\text{eq}}} \right),\end{aligned}\tag{23}$$

where we introduce a dimensionless parameter z which is defined as $z = \frac{M_\eta}{T}$. The equilibrium values for these are expressed as $Y_\eta^{\text{eq}}(z) = \frac{45}{\pi^4 g_*} z^2 K_2(z)$ and $Y_L^{\text{eq}} = \frac{81}{\pi^4 g_*}$, where $K_2(z)$ is the modified Bessel function of the second kind. These equations are derived under the assumption such that the existence of $S_{1,2}$ in the thermal bath can be neglected. It means that both the inverse decay of $S_{1,2}$ and the scattering containing $S_{1,2}$ in the initial and final states do not contribute to these equations. This requires $T_R < m_{S_{1,2}}$ for the reheating temperature T_R . If we take account of eqs. (10) and (21) with it, $\frac{|\mu_1|^2}{m_{S_1}^2} \ll \frac{|\mu_2|^2}{m_{S_2}^2}$ is found to be imposed. Reaction densities $\gamma_{a,b}$ for lepton number conserving scattering processes $\eta\eta \rightarrow \ell_\alpha \ell_\beta$ and $\eta\ell_\alpha^\dagger \rightarrow \eta^\dagger \ell_\beta$ cause the transition of the lepton number asymmetry between the η sector and the doublet lepton sector. On the other hand, reaction densities $\gamma_{x,y}$ for lepton number violating scattering processes $\eta\eta \rightarrow \phi\phi$ and $\eta\phi^\dagger \rightarrow \eta^\dagger \phi$ control the washout of the lepton number asymmetry in the η sector. Formulas of these reaction densities are summarized in Appendix A. If we note that $n_{S_1}(T_R) = \frac{\rho_{S_1}(T_R)}{m_{S_1}}$ and $\rho_{S_1}(T_R) = \frac{\pi^2}{30} g_* T_R^4$ are satisfied for the number density and the energy density of S_1 at T_R under the assumption of instantaneous thermalization, $\Delta Y_\eta(T_R) = \frac{3}{4} \epsilon \frac{T_R}{m_{S_1}}$ could be obtained by using eq. (22). We use it and $\Delta Y_L(T_R) = 0$ as the initial values for this analysis. The lepton number asymmetry ΔY_L obtained at the weak scale as the solution of these Boltzmann equations is converted to the baryon number asymmetry through the sphaleron processes. In the present model, the resulting baryon number asymmetry could be estimated by using the

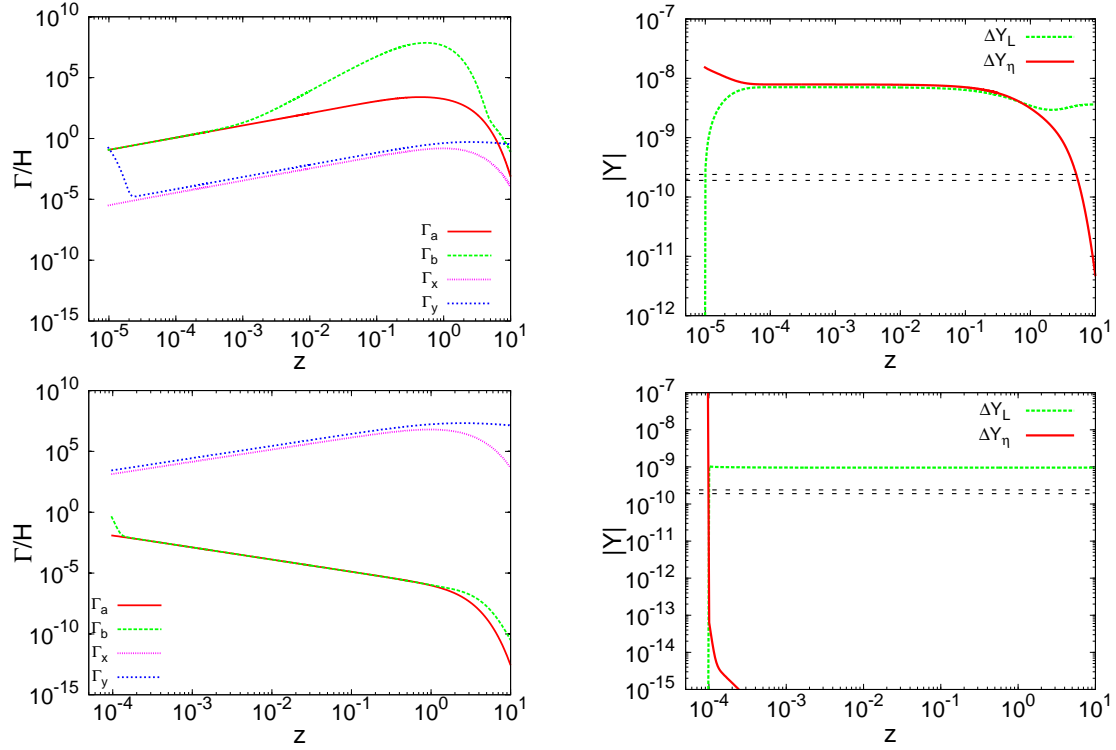


Fig. 3 Relevant reaction rates and solutions of the Boltzmann equations for the cases (a) (upper panels) and (b) (lower panels). They correspond to the cases with single fermion masses of $O(10^4)$ GeV and $O(10^8)$ GeV. In the left-hand panels, the ratio of reaction rate Γ to the Hubble parameter H for the relevant process is plotted as functions of z . In the right-hand panels, the evolution of ΔY_η and ΔY_L are plotted as functions of z . The lepton number asymmetry required to explain the observational results is shown by the horizontal black dashed line.

solution of eq. (23) as¹³

$$Y_B = -\frac{7}{19}\Delta Y_L(z_{EW}). \quad (24)$$

Now we show the results of the numerical analysis of the baryon number asymmetry generated through the scenario described above. Since a factor $\sum_k (hh^\dagger)_{kk}$ is included in the reduced cross section $\hat{\sigma}_{a,b}$ given in Appendix A, we have to determine the flavor structure of neutrino Yukawa couplings for the realistic analysis. We adopt the results obtained in Fig. 2 for it and then they are fixed as

$$(hh^\dagger)_{22} = (1 + q_1^2)h_2^2, \quad (hh^\dagger)_{33} = (1 + q_2^2 + q_3^2)h_3^2, \quad (25)$$

¹³We find a relation $B = -\frac{7}{19}(B - L)$ at the weak scale from the chemical equilibrium condition [17]. Since $B - L$ is conserved under the sphaleron interaction, we note that eq. (23) should be regarded as the Boltzmann equations for it but not for L .

where we could choose the values of $q_{2,3}$ in the allowed region shown in Fig. 2 for $q_1 = 0.77$. In the following analysis, we use $q_2 = -0.4$ and $q_3 = 2.1$ which fix the neutrino oscillation parameters as $\Delta m_{32}^2 = 2.51 \cdot 10^{-3} \text{ eV}^2$, $\Delta m_{21}^2 = 7.63 \cdot 10^{-5} \text{ eV}^2$, $\sin^2 2\theta_{23} = 0.977$, $\sin^2 2\theta_{12} = 0.863$ and $\sin^2 2\theta_{13} = 0.097$. In Fig. 3, we show the solutions obtained for the model parameters given as the cases (a) and (b) in Table 1. For each case, the ratio of the relevant reaction rate to the Hubble parameter is plotted as a function of z in the left panels. The evolution of ΔY_η and ΔY_L is shown in the right panels, where $\Delta Y_L(z_{EW})$ required for the observed baryon number asymmetry is implicated by the horizontal dotted lines. We find that the sufficient amount of baryon number asymmetry is generated for parameters which are consistent with the neutrino oscillation data. The obtained values are listed in the last column of Table 1.

In Fig. 3, we find completely different behavior in the transition of the lepton number asymmetry between the two cases. The difference comes from whether the lepton number conserving scatterings could be in the thermal equilibrium or not. It is determined depending on both values of the neutrino Yukawa couplings and singlet fermion masses. In this model, they are constrained by the neutrino oscillation data together with the value of the effective coupling $\lambda_5 (\simeq \frac{\mu_2^2}{m_{S_2}^2})$ as found in eq. (10). If the lepton number conserving scatterings could be expected in the thermal equilibrium for $T_R \gg M_k$, the situation $\Delta Y_L \simeq \Delta Y_\eta$ is realized during that period. It is found in the case (a). The final value of ΔY_L at the electroweak scale is determined depending on the time when they leave the equilibrium. On the other hand, if we suppose that these processes could never be in the thermal equilibrium, we find that $T_R \ll M_k$ should be satisfied and the relation $\Delta Y_L \simeq \Delta Y_\eta$ cannot be kept during any substantial period. This corresponds to the case (b). The final value of ΔY_L in this case is fixed mainly by the strength of the lepton number conserving scattering processes at T_R .

It is useful to clarify the parameter dependence of the generated baryon number asymmetry Y_B in order to understand this scenario. In the case (a), Y_B is stable against the change of $h_{2,3}$ and $M_{2,3}$ which satisfies the conditions given in eq. (10) as long as λ_5 is kept to be a constant value. This feature is considered to be brought about since the decoupling temperature of the lepton number conserving scatterings is not affected by this variation substantially. On the other hand, Y_B is deeply dependent on the values of μ_1 and μ_2 . The former one determines the initial value of ΔY_η and the latter one controls

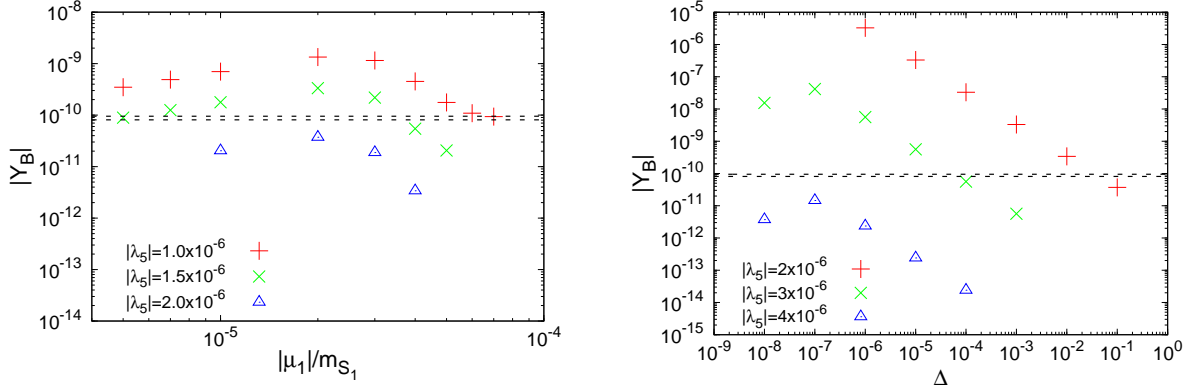


Fig. 4 Left: The dependence of $|Y_B|$ on $\frac{|\mu_1|}{m_{S_1}}, \frac{|\mu_2|}{m_{S_2}} (\simeq \sqrt{|\lambda_5|})$ which are relevant to the initial value of the lepton number asymmetry and the washout of the lepton number asymmetry, respectively. $m_{S_2} = 1.1m_{S_1}$ is assumed. Right: The dependence of $|Y_B|$ on $\Delta \equiv \frac{m_{S_2}}{m_{S_1}} - 1$ for several values of $|\lambda_5|$. $\frac{|\mu_1|}{m_{S_1}} = 2 \cdot 10^{-5}$ is assumed. In both panels, other parameters are fixed to satisfy the neutrino oscillation data assuming $m_{S_1} = 10^9$ GeV and $M_\eta = 1$ TeV as discussed in the part relevant to eq. (10).

the washout of ΔY_η . Examples of this dependence could be seen are through the left panel of Fig. 4. Smaller $|\mu_1|$ makes the reheating temperature T_R lower and then reduces the initial lepton number asymmetry $\Delta Y_\eta(T_R)$. Larger $|\mu_1|$ makes T_R higher and T_R could take a near value to $m_{S_{1,2}}$ in the present setting. This makes the washout of ΔY_η at the neighborhood of T_R be enhanced due to the tail effect of the s -channel resonance. It can be seen at a small z region in the figures of $\frac{\Gamma}{H}$. These could explain the reason why $|Y_B|$ is a convex function of $\frac{|\mu_1|}{m_{S_1}}$. Since larger $|\lambda_5|$ makes the washout effect larger as found from the formulas of $\hat{\sigma}_{x,y}$ given in Appendix A, $|\lambda_5|$ is expected to have an upper bound. The left panel of Fig. 4 shows that $|\lambda_5|$ should be smaller than $2 \cdot 10^{-6}$ to guarantee the sufficient amount of $|Y_B|$ in this case. Degeneracy between m_{S_1} and m_{S_2} is also crucial to fix the value of the CP asymmetry and then the initial lepton number asymmetry $\Delta Y_\eta(T_R)$. In the right panel of Fig. 4, $|Y_B|$ is plotted as a function of $\Delta (\equiv \frac{m_{S_2}}{m_{S_1}} - 1)$. If the mass difference becomes smaller, the second term in eq. (22) which comes from the self-energy diagram is enhanced and then the initial value of $\Delta Y_\eta(T_R)$ becomes larger. However, as shown in these examples, the fine degeneracy is not required as long as λ_5 takes a smaller value as mentioned above. It is a distinctive point from the ordinary TeV scale thermal leptogenesis. This comes from the non-thermal origin due to the inflation decay which could prepare a sufficient amount of asymmetry.

In the case (b), the situation is completely different from the case (a). Y_B is largely dependent on the setting of $h_{2,3}$ and $M_{2,3}$ for a fixed value of λ_5 . Unless M_k is much larger than T_R , the rate of the lepton number conserving scatterings could be enhanced to be almost in the thermal equilibrium at the neighborhood of T_R . In that case, since the washout processes are in the equilibrium due to an assumed large value of $|\lambda_5|$, ΔY_η decreases steeply and the transferred ΔY_L follows ΔY_η not to reach a substantial value. To escape this situation, it seems to be necessary for M_k to be larger than T_R by an order of magnitude at least. These features clarify how both $\frac{\mu_1}{m_{S_1}}$ and $\frac{\mu_2}{m_{S_2}}$ play crucial roles in this scenario. Anyway, these studies suggest that the present non-thermal leptogenesis could give us a successful scenario for the generation of the baryon number asymmetry. It is completely consistent with the neutrino mass generation which could explain all the neutrino oscillation data.

4.2 Dark matter

In this subsection, we discuss the connection between this leptogenesis scenario and DM physics under the assumption that the lightest neutral scalar η_R^0 is DM. At first, we discuss the relic abundance of η_R^0 . In the mass range of η_R^0 discussed in this paper, its abundance is known to be determined by the couplings $\lambda_{3,4}$ in eq. (1) [11, 12], which are completely irrelevant to the analysis of other phenomena studied here.¹⁴ As discussed in [30], the lepton number asymmetry kept in the η sector cannot play any role in the DM abundance. The asymmetry in this sector disappears through the effective coupling λ_5 after the electroweak symmetry breaking. Thus, the required relic abundance should be realized as thermal relics for suitable values of $\lambda_{3,4}$. The estimation of its relic abundance for $M_\eta = 600$ GeV, 1 and 3 TeV is shown in Fig. 5, which is obtained by using the ordinary method whose detail can be found in [30]. Since the required abundance is displayed by the horizontal dotted line in this figure, we find that appropriate values of $\lambda_{3,4}$ could make the thermal η_R^0 be a favorable DM candidate naturally.

Next, we discuss the consistency between this leptogenesis scenario and the η_R^0 DM. Since the effective coupling $\lambda_5 (\simeq \frac{\mu_2^2}{m_{S_2}^2})$ takes a small value, the real and imaginary parts $\eta_{R,I}^0$ of the neutral component of η have almost degenerate masses whose difference is

¹⁴We note that the required relic abundance cannot be explained for $M_{\eta_R^0} \lesssim 530$ GeV where only the gauge interaction reduces it below the required value [12].

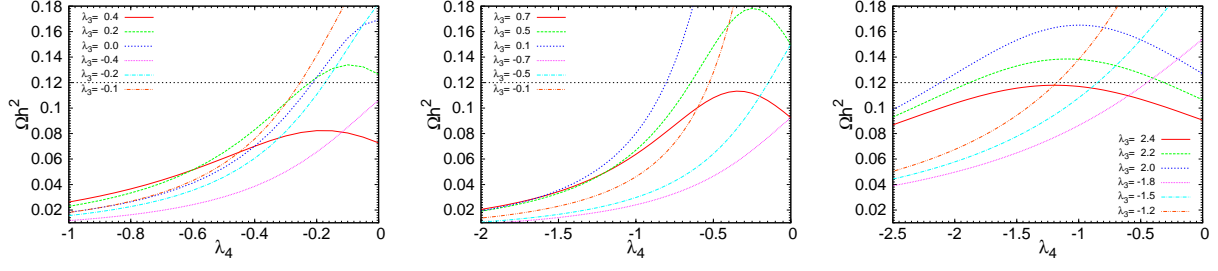


Fig. 5 Thermal η_R^0 relic abundance for $M_\eta = 600$ GeV, 1 TeV and 3 TeV from the left to the right, respectively. It is estimated by taking account of the coannihilation between the components of η which is controlled by the couplings $\lambda_{3,4}$.

expressed as¹⁵

$$\delta \equiv M_{\eta_I^0} - M_{\eta_R^0} = \frac{\langle \phi \rangle^2}{M_\eta} \frac{\mu_2^2}{m_{S_2}^2}. \quad (26)$$

On the other hand, η_R^0 and η_I^0 have a weak gauge interaction such as

$$\mathcal{L}_{\text{int}} = \frac{g}{2} Z^\mu (\eta_R \partial_\mu \eta_I - \eta_I \partial_\mu \eta_R). \quad (27)$$

This interaction induces the spin-independent inelastic scattering $\eta_R N \rightarrow \eta_I N$ with a nucleus N mediated by a Z^0 exchange in which the nucleus is not excited as long as the mass difference δ is sufficiently small. This reaction can contribute to the direct search of DM. The η_R^0 -nucleon cross section for this inelastic scattering can be estimated as

$$\sigma_{n,\text{inel}}^0 = \frac{G_F^2}{2\pi\mu_n^2} \simeq 7.44 \times 10^{-39} \text{ cm}^2, \quad (28)$$

where μ_n is the reduced mass of this η_R^0 -nucleon system and $\delta \ll M_\eta$ is assumed. If we apply the bound from recent DM direct search experiments to this cross section, we could approximately derive a useful constraint on this leptogenesis scenario.

As briefly described the in Appendix B, the present bound on σ_n^0 estimated for the elastic scattering ($\delta = 0$) might be translated to the one for the inelastic scattering ($\delta \neq 0$) as

$$\sigma_{n,\text{inel}}^0 = \sigma_{n,\text{el}}^0 \frac{\int_{v_{\min}(\delta=0)}^{v_{\text{esc}}} dv \left(e^{-\frac{(v-v_e)^2}{v_0^2}} - e^{-\frac{(v+v_e)^2}{v_0^2}} \right)}{\int_{v_{\min}(\delta \neq 0)}^{v_{\text{esc}}} dv \left(e^{-\frac{(v-v_e)^2}{v_0^2}} - e^{-\frac{(v+v_e)^2}{v_0^2}} \right)}, \quad (29)$$

¹⁵ η_R^0 and η_I^0 could be mass eigenstates for a real λ_5 . Since we assume that μ_2 is real and $\frac{|\mu_1|^2}{m_{S_1}^2} \ll \frac{|\mu_2|^2}{m_{S_2}^2}$ is satisfied, the effective coupling λ_5 can be treated as a real parameter.

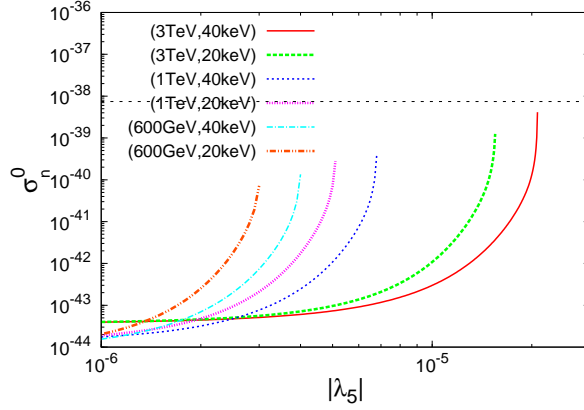


Fig. 6 Constraint on the effective coupling λ_5 , which is derived from the DM direct detection experiments. Each line represents $\sigma_{n,\text{inel}}^0$ for (M_η, E_R) . A bound for σ_n^0 at $m_{\text{DM}} = 3 \text{ TeV}$, 1 TeV and 600 GeV given by LUX is used.

where v_{min} is the minimum η_R^0 velocity required to induce this scattering. This $\sigma_{n,\text{inel}}^0$ obtained by using the present bound on σ_n^0 should be larger than the value given in eq. (28) since DM has not been detected in any direct detection experiments [32, 33]. We also note that η_R^0 cannot be detected in any direct search experiments unless $v_{\text{min}} < v_{\text{esc}}$ is satisfied for the local escape velocity v_{esc} from our Galaxy. It is estimated as $498 \text{ km/s} < v_{\text{esc}} < 608 \text{ km/s}$ [34] and its medium value 544 km/s is used as v_{esc} in this analysis. In Fig. 6, we plot $\sigma_{n,\text{inel}}^0$ corresponding to it as a function of $|\lambda_5|$ for typical values of the recoil energy of nucleus E_R by using the bound of σ_n^0 given by LUX [33] as $\sigma_{n,\text{el}}^0$ in eq. (29).¹⁶ Since the endpoint of each line represents the occurrence of $v_{\text{min}} = v_{\text{esc}}$, the scattering is kinematically forbidden at the larger $|\lambda_5|$ region than it and then such a region of $|\lambda_5|$ is allowed from the result of the present direct DM search. Unless the escape velocity takes much larger values than the one used here, this analysis unfortunately suggests that this DM with the mass $M_\eta \lesssim 6 \text{ TeV}$ is difficult to be detected through this inelastic scattering process in the direct search experiments.

If we take account of the relation $|\lambda_5| \simeq \frac{|\mu_2|^2}{m_{S_2}}$ in this model, we might roughly read off

¹⁶Since the differential WIMP-nucleus cross section in the case of scattering leading to a heavier WIMP depends on the recoil energy very differently from that associated with the standard elastic scattering and since in the present case the nucleon cross section depends on the WIMP velocity, clearly we cannot derive an exact bound by using the experimental result for the elastic scattering.

the condition required from this figure as follows,

$$\frac{\mu_2^2}{m_{S_2}^2} \gtrsim \begin{cases} (1-2) \times 10^{-5} & \text{for } M_{\eta_R^0} = 3 \text{ TeV}, \\ (5-7) \times 10^{-6} & \text{for } M_{\eta_R^0} = 1 \text{ TeV}, \\ (3-4) \times 10^{-6} & \text{for } M_{\eta_R^0} = 600 \text{ GeV}, \end{cases} \quad (30)$$

although it has non-negligible dependence on E_R and v_{esc} . We should note that $|\lambda_5|$ cannot take small values freely even if the neutrino mass constraints have only to be satisfied. In the case (b), this constraint is found to be consistent with the parameters used in the above analysis of the baryon number asymmetry. On the other hand, in the case (a), one might consider from Fig. 6 that this constraint is not satisfied and the scenario is inconsistent. However, it may be appropriate to judge that the consistency of the parameters used here is marginal if we take account of several uncertainties included in the estimation of the bound on $|\lambda_5|$. We also note that the situation could be improved if we suppose fine mass degeneracy between S_1 and S_2 such as $\Delta = 10^{-6}$ and a favorable value for $\frac{|\mu_1|}{m_{S_1}}$ such as $2 \cdot 10^{-5}$. As we find in the right-panel of Fig. 5, these could enhance the initial asymmetry of the lepton number produced through the inflaton decay. In this case, for example, $|Y_B| = 1.2 \cdot 10^{-10}$ can be obtained for $|\lambda_5| = 3.5 \cdot 10^{-6}$ at $M_\eta = 1 \text{ TeV}$.

5 Summary

We have proposed an extension of the radiative neutrino mass model with Z_2 odd real singlet scalars, which give a seed of lepton number violation to allow Majorana neutrino mass generation at one-loop level. If they have hierarchical non-minimal couplings with the Ricci scalar such as $\sum_a \xi_a S_a^2 R$ with $\xi_1 \gg 1 \gg \xi_2$, the S_1 potential at large field regions is so flat that sufficient inflation could be induced. Although both the scalar spectral index and the tensor-to-scalar ratio take favorable values just as the Higgs inflation, the model can evade from the unitarity problem differently from the ordinary Higgs inflation. Since the unitarity violating scale could be similar to or larger than the inflation scale, the flatness of the inflaton potential is never disturbed by new physics which restores the unitarity of the model.

The decay of inflaton could non-thermally produce the lepton number asymmetry in the η sector through the reheating processes. Although its decay cannot yield this asymmetry directly in the lepton sector, the lepton number conserving scatterings could

convert a sufficient amount of asymmetry from the η sector to the lepton sector. This lepton number asymmetry is transferred to the baryon number asymmetry through the sphaleron interaction. Parameters relevant to this leptogenesis are constrained by the neutrino oscillation data and the DM direct search experiments. We have shown that the sufficient baryon number could be generated consistently with these constraints under suitable conditions. Moreover, the DM abundance could be fixed by the parameters which are irrelevant to all of these as long as η_R^0 is supposed to be DM. Although the model considered here is very simple, it can compactly explain problems in the SM such as the neutrino mass generation, the DM origin and its abundance, the inflation and the baryon number asymmetry in the Universe. They are closely related each other through the radiative mechanism for the neutrino mass generation.

Acknowledgements

R. H. S. Budhi is supported by the Directorate General of Higher Education (DGHE) of Indonesia (Grant Number 1245/E4.4/K/2012). S. K. is supported by Grant-in-Aid for JSPS fellows (26·5862). D. S. is supported by MEXT Grant-in-Aid for Scientific Research on Innovative Areas (Grant Number 26104009).

Appendix A

We summarize the formulas for the reaction densities which contribute to the Boltzmann equations used in this analysis. We introduce dimensionless variables

$$x = \frac{s}{M_\eta^2}, \quad a_k = \frac{M_k^2}{M_\eta^2}, \quad b_a = \frac{m_{S_a}^2}{M_\eta^2}, \quad c_a = \frac{|\mu_a|^2}{M_\eta^2}, \quad (31)$$

where s is the squared center of mass energy. The reaction density for the scattering processes is expressed as

$$\gamma(ab \rightarrow ij) = \frac{T}{64\pi^4} \int_{s_{\min}}^{\infty} ds \, \hat{\sigma}(s) \sqrt{s} K_1 \left(\frac{\sqrt{s}}{T} \right), \quad (32)$$

where $\hat{\sigma}(s)$ is the reduced cross section and $K_1(z)$ is the modified Bessel function of the second kind. The lower bound of integration is defined as $s_{\min} = \max[(m_a + m_b)^2, (m_i + m_j)^2]$.

The reduced cross section $\hat{\sigma}_{a,b}$ for the lepton number conserving scattering processes are given as

$$\begin{aligned} \hat{\sigma}_a(x) = & \frac{1}{2\pi} \left[\sum_{k=1}^3 (hh^\dagger)_{kk}^2 \left\{ \frac{a_k(x^2 - 4x)^{1/2}}{a_k x + (a_k - 1)^2} \right. \right. \\ & + \frac{a_k}{x + 2a_k - 2} \ln \left(\frac{x + (x^2 - 4x)^{1/2} + 2a_k - 2}{x - (x^2 - 4x)^{1/2} + 2a_k - 2} \right) \Big\} \\ & + \sum_{i>j} \frac{\text{Re}[(hh^\dagger)_{ij}^2] \sqrt{a_i a_j}}{x + a_i + a_j - 2} \left\{ \frac{2x + 3a_i + a_j - 4}{a_j - a_i} \ln \left(\frac{x + (x^2 - 4x)^{1/2} + 2a_i - 2}{x - (x^2 - 4x)^{1/2} + 2a_i - 2} \right) \right. \\ & \left. \left. + \frac{2x + a_i + 3a_j - 4}{a_i - a_j} \ln \left(\frac{x + (x^2 - 4x)^{1/2} + 2a_j - 2}{x - (x^2 - 4x)^{1/2} + 2a_j - 2} \right) \right\} \right] \end{aligned} \quad (33)$$

for $\eta\eta \rightarrow \ell_\alpha \ell_\beta$ and

$$\begin{aligned} \hat{\sigma}_b(x) = & \frac{1}{2\pi} \frac{(x-1)^2}{x^2} \left[\sum_{k=1}^3 (hh^\dagger)_{kk}^2 \frac{a_k}{x} \left\{ \frac{x^2}{x a_k - 1} + \frac{2x}{D_k(x)} + \frac{(x-1)^2}{2D_k(x)^2} \right. \right. \\ & - \frac{x^2}{(x-1)^2} \left(1 + \frac{2(x + a_k - 2)}{D_k(x)} \right) \ln \left(\frac{x(x + a_k - 2)}{x a_k - 1} \right) \Big\} \\ & + \sum_{i>j} \text{Re}[(hh^\dagger)_{ij}^2] \frac{\sqrt{a_i a_j}}{x} \left\{ \frac{x}{D_i(x)} + \frac{x}{D_j(x)} + \frac{(x-1)^2}{D_i(x) D_j(x)} \right. \\ & + \frac{x^2}{(x-1)^2} \left(\frac{2(x + a_i - 2)}{a_j - a_i} - \frac{x + a_i - 2}{D_j(x)} \right) \ln \frac{x(x + a_i - 2)}{x a_i - 1} \\ & \left. \left. + \frac{x^2}{(x-1)^2} \left(\frac{2(x + a_j - 2)}{a_i - a_j} - \frac{x + a_j - 2}{D_i(x)} \right) \ln \frac{x(x + a_j - 2)}{x a_j - 1} \right\} \right] \end{aligned} \quad (34)$$

for $\eta\ell_\alpha^\dagger \rightarrow \eta^\dagger\ell_\beta$. In these formulas, we use the following definition for convenience:

$$\frac{1}{D_k(x)} = \frac{x - a_k}{(x - a_k)^2 + a_k^2 d_k}, \quad d_k = \frac{1}{64\pi^2} \left(\sum_{\alpha=e,\mu,\tau} |h_{\alpha k}|^2 \right)^2 \left(1 - \frac{1}{a_k} \right)^4. \quad (35)$$

If we take account of the assumption $\frac{|\mu_1|^2}{m_{S_1}^2} \ll \frac{|\mu_2|^2}{m_{S_2}^2}$, the reduced cross section $\hat{\sigma}_{x,y}$ of the lepton number violating scattering processes could be approximately represented as

$$\begin{aligned} \hat{\sigma}_x(x) &\simeq \frac{c_2^2}{\pi} \frac{1}{(x^3(x-4))^{1/2}} \left(\frac{2}{P_2^2-1} + \frac{1}{P_2} \ln \frac{P_2+1}{P_2-1} \right), \\ \hat{\sigma}_y(x) &\simeq \frac{c_2^2}{\pi} \left[\frac{2}{(x-1)^2} \frac{1}{Q_2^2-1} + \frac{(x-1)^2}{2x^2} \frac{1}{\tilde{D}_2(x)} + \frac{1}{x} \frac{x-b_2}{\tilde{D}_2(x)} \ln \frac{Q_2+1}{Q_2-1} \right] \end{aligned} \quad (36)$$

for $\eta\eta \rightarrow \phi\phi$ and $\eta\phi^\dagger \rightarrow \eta^\dagger\phi$, respectively. In these formulas we use the definition such as

$$\begin{aligned} \frac{1}{\tilde{D}_a(x)} &= \frac{1}{(x - b_a)^2 + b_a^2 \tilde{d}_a}, \quad \tilde{d}_a = \frac{1}{64\pi^2} \left(\frac{c_a}{b_a} \right)^2 \left(1 - \frac{1}{b_a} \right)^2, \\ P_a &= \frac{2(1 - b_a) - x}{[x(x-4)]^{1/2}}, \quad Q_a = -1 + \frac{2(1 - xb_a)}{(x-1)^2}. \end{aligned} \quad (37)$$

Appendix B

We consider the direct DM detection through the inelastic scattering with the target composed of the nucleus with the atomic number Z and the mass number A [35, 36]. Its differential detection rate per unit target mass is

$$\frac{dR}{dE_R} = N_T \frac{\rho_{\text{DM}}}{m_{\text{DM}}} \int d^3v \, v f(\vec{v}, \vec{v}_e) \frac{d\sigma}{dE_R}, \quad (38)$$

where N_T is a number of target nuclei per unit mass and E_R is the recoil energy of nucleus. The DM velocity distribution in the rest frame of detector may be taken as a Maxwell-Boltzmann distribution $f(\vec{v}, \vec{v}_e) = \frac{1}{(\pi v_0^2)^{3/2}} \exp\left(-\frac{(\vec{v}+\vec{v}_e)^2}{v_0^2}\right)$ with $v_0 = 220$ km/s. We take into account the motion of the Sun and the Earth by using \vec{v}_e whose magnitude changes as $v_e = v_0 \left[1.05 + 0.07 \cos\left(\frac{2\pi(t-t_p)}{1 \text{ yr}}\right) \right]$. The minimum velocity for which the scattering can occur is estimated as

$$v_{\min} = \frac{1}{\sqrt{2m_N E_R}} \left(\frac{m_N E_R}{m_r} + \delta \right), \quad (39)$$

where m_N is the mass of a target nucleus and m_r is the reduced mass of DM-nucleus system $m_r = \frac{m_{\text{DM}} m_N}{m_{\text{DM}} + m_N}$. The differential cross section $\frac{d\sigma}{dE_R}$ for spin independent interaction

is expressed by using the DM-nucleon cross section σ_n^0 at zero momentum transfer as

$$\frac{d\sigma}{dE_R} = \frac{m_N}{2v^2\mu_n^2} \frac{[Zf_p + (A-Z)f_n]^2}{f_n^2} \sigma_n^0 F^2(E_R), \quad (40)$$

where $F(E_R)$ is a form factor of the nucleus. If we substitute this in eq. (38), the differential rate can be represented by using eq. (40) as

$$\frac{dR}{dE_R} = D_N \sigma_n^0 \int d^3v \frac{1}{v} f(\vec{v}, \vec{v}_e), \quad (41)$$

where D_N is written as

$$D_N = N_T \frac{m_N \rho_{\text{DM}}}{2\mu_n^2 m_{\text{DM}}} \frac{[Zf_p + (A-Z)f_n]^2}{f_n^2} F^2(E_R). \quad (42)$$

We note that D_N takes a fixed value as long as the same target is used.

The remaining part depends on the sub-process and it can be expressed as

$$\sigma_n^0 \int dv \frac{1}{v^2} f(\vec{v}, \vec{v}_e) = \sigma_n^0 \frac{1}{\sqrt{\pi} v_0 v_e} \int_{v_{\min}}^{v_{\text{esc}}} dv \left(e^{-\frac{(v-v_e)^2}{v_0^2}} - e^{-\frac{(v+v_e)^2}{v_0^2}} \right). \quad (43)$$

This depends on whether the scattering occurs elastically ($\delta = 0$) or inelastically ($\delta \neq 0$). If we interpret the present direct detection results based on these scattering processes, the present bound on the elastic scattering cross section $\sigma_{n,\text{el}}^0$ can be translated to the bound on the inelastic scattering cross section $\sigma_{n,\text{inel}}^0$ through

$$\sigma_{n,\text{inel}}^0 \int_{v_{\min}(\delta \neq 0)}^{v_{\text{esc}}} dv \left(e^{-\frac{(v-v_e)^2}{v_0^2}} - e^{-\frac{(v+v_e)^2}{v_0^2}} \right) = \sigma_{n,\text{el}}^0 \int_{v_{\min}(\delta=0)}^{v_{\text{esc}}} dv \left(e^{-\frac{(v-v_e)^2}{v_0^2}} - e^{-\frac{(v+v_e)^2}{v_0^2}} \right). \quad (44)$$

We use this relation to constrain the allowed values of δ , which makes us possible to find the lower bound of the effective coupling $|\lambda_5|$.

References

- [1] ATLAS Collaboration, G. Aad, *et al.*, Phys. Lett. **B716** (2012) 1; CMS Collaboration, S. Chatrchyan, *et al.*, Phys. Lett. **B716** (2012) 30.
- [2] Super-Kamiokande Collaboration, Y. Fukuda, *et al.*, Phys. Rev. Lett. **81** (1998) 1562; SNO Collaboration, Q. R. Ahmad, *et al.*, Phys. Rev. Lett. **89** (2002) 011301; KamLAND Collaboration, K. Eguchi, *et al.*, Phys. Rev. Lett. **90** (2003) 021802; K2K Collaboration, M. H. Ahn, *et al.*, Phys. Rev. Lett. **90** (2003) 041801; T2K Collaboration, K. Abe, *et al.*, Phys. Rev. Lett. **107** (2011) 041801; Double Chooz Collaboration, Y. Abe, *et al.*, Phys. Rev. Lett. **108** (2012) 131801; RENO Collaboration, J. K. Ahn, *et al.*, Phys. Rev. Lett. **108** (2012) 191802; The Daya Bay Collaboration, F. P. An, *et al.*, Phys. Rev. Lett. **108** (2012) 171803.
- [3] WMAP Collaboration, D. N. Spergel, *et al.*, Astrophys. J. **148** (2003) 175; SDSS Collaboration, M. Tegmark, *et al.*, Phys. Rev. **D69** (2004) 103501.
- [4] A. Riotto and M. Trodden, Ann. Rev. Nucl. Part. Sci. **49** (1999) 35; W. Bernreuther, Lect. Notes Phys. **591** (2002) 237; M. Dine and A. Kusenko, Rev. Mod. Phys. **76** (2003) 1.
- [5] E. Ma, Phys. Rev. **D73** (2006) 077301.
- [6] J. Kubo, E. Ma and D. Suematsu, Phys. Lett. **B642** (2006) 18.
- [7] D. Suematsu, T. Toma and T. Yoshida, Phys. Rev. **D79** (2009) 093004; D. Suematsu, T. Toma and T. Yoshida, Phys. Rev. **D82** (2010) 013012.
- [8] J. Kubo and D. Suematsu, Phys. Lett. **B643** (2006) 336.
- [9] D. Aristizabal Sierra, J. Kubo, D. Restrepo, D. Suematsu and O. Zapata, Phys. Rev. **D79** (2009) 013011; E. Ma, Annals Fond. Broglie **31** (2006) 285; H. Fukuoka, J. Kubo and D. Suematsu, Phys. Lett. **B678** (2009) 401; D. Suematsu and T. Toma, Nucl. Phys. **B847** (2011) 567; H. Fukuoka, D. Suematsu and T. Toma, JCAP **07** (2011) 001.
- [10] D. Suematsu, Eur. Phys. J. **C56** (2008) 379; H. Higashi, T. Ishima and D. Suematsu, Int. J. Mod. Phys. **A26** (2011) 995; D. Suematsu, Eur. Phys. J. **C72** (2012) 1951.

- [11] S. Kashiwase and D. Suematsu, Phys. Rev. **D86** (2012) 053001; S. Kashiwase and D. Suematsu, Eur. Phys. J. **C73** (2013) 2484.
- [12] L. L. Honorez, E. Nezri, J. F. Oliver and M. H. G. Tytgat, JCAP **02** (2007) 028; T. Hambye, F.-S. Ling, L. L. Honorez and J. Rocher, JHEP **07** (2009) 090.
- [13] Planck Collaboration, P. A. R. Ade, *et al.*, arXiv1303.5082 [astro-ph.CO].
- [14] BICEP2/Keck and Planck Collaborations, P. A. R. Ade, *et al.*, arXiv:1502.00612 [astro-ph].
- [15] Planck Collaboration, P. A. R. Ade, *et al.*, arXiv:1502.01589 [astro-ph.CO]; Planck Collaboration, P. A. R. Ade, *et al.*, arXiv:1502.02114 [astro-ph.CO].
- [16] F. Bezrukov and M. Shaposhnikov, Phys. Lett. **B659** (2008) 703; F. L. Bezrukov, A. Magnin and M. Shaposhnikov, Phys. Lett. **B675** (2009) 88.
- [17] D. Suematsu, Phys. Rev. **D85** (2012) 073008.
- [18] R. N. Lerner and J. McDonald, Phys. Rev. **D80** (2009) 123507; R. N. Lerner and J. McDonald, Phys. Rev. **D83** (2011) 123522.
- [19] J. L. F. Barbón and J. R. Espinosa, Phys. Rev. **D79** (2009) 081302(R); C. P. Burgess, H. M. Lee and M. Trott, JHEP **1007** (2010) 007; M. P. Hertzberg, JHEP **1011** (2010) 023; D. I. Kaiser, Phys. Rev. **D81** (2010) 084044.
- [20] R. N. Lerner and J. McDonald, JCAP **11** (2012) 019.
- [21] K. A. Olive, *et al.* (Particle Data Group), Chin. Phys. C, 38 (2014) 090001.
- [22] R. H. S. Budhi, S. Kashiwase and D. Suematsu, Phys. Rev. **D90** (2014) 113013; R. H. S. Budhi, S. Kashiwase and D. Suematsu, JCAP **09** (2015) 039.
- [23] B. L. Spokoiny, Phys. Lett. **B147** (1984) 39; D. S. Salopek, J. R. Bond and J. M. Bardeen, Phys. Rev. **D40** (1989) 1753.
- [24] A. De Simone, M. P. Hertzberg and F. Wilczek, Phys. Lett. **B678** (2009) 1; G. F. Giudice and H. M. Lee, Phys. Lett. **B694** (2011) 294; F. Bezrukov, A. Magnin, M. Shaposhnikov and S. Sibiryakov, JHEP **1101** (2011) 016; R. N. Lerner and J. McDonald, Phys. Rev. **D83** (2011) 123522; J. Elias-Miró, J. R. Espinosa, G. F. Giudice,

- G. Isidori, A. Riotto and A. Strumia, Phys. Lett. **B709** (2012) 222; X. Calmet and R. Casadio, Phys. Lett. **B734** (2014) 17.
- [25] J.-O. Gong, H. M. Lee and S. K. Kang, JHEP **1204** (2012) 128; S. Kanemura, T. Matsui and T. Nabeshima, Phys. Lett. **B723** (2013) 126.
- [26] For reviews, D. H. Lyth and A. Riotto, Phys. Rept. **314** (1999) 1; A. R. Liddle and D. H. Lyth, *Cosmological inflation and Large-Scale Structure* (Cambridge University Press, 2000).
- [27] S. Davidson and A. Ibarra, Phys. Lett. **B535** (2002) 25.
- [28] M. Flanz, E. A. Paschos and U. Sarkar, Phys. Lett. **B345** (1995) 248; L. Covi, E. Roulet and F. Vissani, Phys. Lett. **B384** (1996) 169; E. Akhmedov, M. Frigerio and A. Yu Smirnov, JHEP **0309** (2003) 021; C. H. Albright and S. M. Barr, Phys. Rev. **D69** (2004) 073010; T. Hambye, J. March-Russell and S. M. West, JHEP **0407** (2004) 070.
- [29] A. Pilaftsis and T. E. J. Underwood, Nucl. Phys. **B692** (2004) 303; A. Pilaftsis and T. E. J. Underwood, Phys. Rev. **D72** (2005) 113001.
- [30] S. Kashiwase and D. Suematsu, Phys. Lett. **B749** (2015) 603.
- [31] G. Lazarides and Q. Shafi, Phys. Lett. **B258** (1991) 305.
- [32] G. Angloher *et al.*, Astropart. Phys. **31** (2009) 270; V. N. Lebedenko *et al.*, Phys. Rev. **D80** (2009) 052010; CDMS Collaboration, Z. Ahmed, *et al.*, Phys. Rev. Lett. **102** (2009) 011301; The XENON100 Collaboration, E. Aprile, *et al.*, Phys. Rev. Lett. **105** (2010) 131302; The XENON100 Collaboration, E. Aprile, *et al.*, Phys. Rev. Lett. **109** (2012) 181301.
- [33] LUX Collaboration, D. S. Akerib *et al.*, Phys. Rev. Lett. **112** (2014) 091303.
- [34] M. C. Smith, *et al.*, Mon. Not. R. Astron. Soc. **379** (2007) 755.
- [35] F. J. Petriello and K. M. Zurek, JHEP **0809** (2008) 047; Y. Cui, D. E. Marrissey, D. Poland and L. Randall, JHEP **0905** (2009) 076; C. Arina, F.-S. Ling and M. H. G. Tytgat, JCAP **0910** (2009) 018; S. Chang, G. D. Kribs, D. Tucker-Smith and N. Weiner, Phys. Rev. **D79** (2009) 043513.

[36] The XENON100 Collaboration, E. Aprile, *et al.*, Phys. Rev. **D84** (2011) 061101(R).